Catalysis Today 205 (2013) 34–40

Contents lists available at SciVerse ScienceDirect

Catalysis Today

journal homepage: www.elsevier.com/locate/cattod

Selective detection of reaction intermediates using concentration-modulation excitation DRIFT spectroscopy

Alejo Aguirre, Sebastián E. Collins*

Instituto de Desarrollo Tecnológico para la Industria Química (INTEC), Universidad Nacional del Litoral, CONICET. Güemes 3450, S3000GLN, Santa Fe, Argentina

ARTICLE INFO

Article history:
Received 20 June 2012
Received in revised form 14 August 2012
Accepted 16 August 2012
Available online 19 September 2012

Keywords:
DRIFT
Modulation excitation spectroscopy
Palladium-gallia
Formates
Reverse water gas shift reaction

ABSTRACT

Concentration-modulation excitation spectroscopy (MES) experiments in combination with phase-sensitive detection (PSD) were used to monitor the gas–solid interface by means of *in operando* diffuse reflectance infrared spectroscopy (DRIFT). The MES methodology is a powerful technique because it allows sensitive and selective spectroscopic detection and monitoring of the dynamic behavior of species directly involved in a reaction.

In this work, c-MES was employed to monitor the adsorption of hydrogen and carbon dioxide and their reaction (reverse water gas shift) on a model Pd(1 wt.%)/γ-Ga_2O_3 catalyst. Details of the reaction mechanism could be reached: (i) H_2 is dissociatively chemisorbed on the gallium oxide surface giving Ga–H species; (ii) CO_2 is adsorbed giving rise of carbonate groups; (iii) on the gallia surface, carbonates are hydrogenated by Ga–H to produce formate species with different coordination, e.g. monodentate, bidentate and bridged formates, which in turn are decomposed into CO(g); (iv) the metal phase increases the formate surface concentration onto the gallia because of an efficient supply of atomic hydrogen via a spillover. Results also indicated that monodentate formates are the most reactive intermediate.

1. Introduction

Fourier transformed infrared (FTIR) spectroscopy is an appropriated technique for the investigation of reaction pathways in heterogeneous catalytic systems because it provides the detection of species adsorbed on a catalyst under reaction conditions (*Operando* mode) [1–5]. Thus, increasing efforts to implement cells/microreactors to spectroscopically assess the gas(reactant)/solid(catalyst) interface, while simultaneously measuring activity and selectivity, have been carried out by several research groups [6–8]. However, the presence of strongly absorbent solvents, spectator species and/or the catalyst itself can make very difficult or preclude the identification and tracking of the true active species, that is, the intermediates. Then, transient experiments are widely applied in the analysis of reaction intermediates by perturbing a catalytic system working under steady state conditions (*ss*). Moreover, studies have been successfully performed by DRIFT coupled with steady state isotopic transient kinetics analysis (SSITKA), for instance, on the direct and reverse WGS reaction, obtaining not only activity data, but also making possible to distinguish between different surface intermediaries and those who are spectators of the reaction [2,9]. Rigorously, the DRIFT–SSITKA studies are so far a unique tool to differentiate objectively between intermediate and spectators under *operando* conditions because during the isotopic exchange the chemical potential is (almost) kept constant [10]. However, isotopic exchange techniques are limited to relatively simple reactions (reactants and products with "few atoms") since in more complex reactions possible combinations of isotopic exchange among reactants and products (scrambling) extremely complicate the analysis of the results [11]. In addition, the economic factor cannot be ignored, since the cost of isotopically labeled reagents is considerably high.

Modulated experiments have proved to be an adequate methodology to perform qualitative and quantitative analysis of reaction mechanisms [12–14]. Modulation excitation spectroscopy (MES) is based on the disturbance of a system operated under *ss* by the periodical variation of an external parameter such as temperature, pressure, or concentration of a reactant. Therefore, all the species in the system that are affected by this external parameter will also change periodically with the same frequency of the perturbation, but with a phase lag. This phase lag implicitly contains the kinetic constant of an elemental reaction step [15,16]. MES applied to *in operando* DRIFT experiments is a powerful tool which can allow the sensitive and selective detection of species directly involved in a reaction at the gas–solid interface, and the monitoring of their dynamic behaviors. Moreover, combined with phase sensitive detection (PSD) method, it allows to separate a weak response from a strong background signal [12].

* Corresponding author.
E-mail address: scollins@santafe-conicet.gov.ar (S.E. Collins).

0920-5861/$ – see front matter © 2012 Elsevier B.V. All rights reserved.
http://dx.doi.org/10.1016/j.cattod.2012.08.020

Thus, small perturbations around the *ss* (that is, maintaining almost constant the concentrations of reactants) can be used to identify and to follow selectively the reaction surface intermediates under real reaction conditions (*in operando*).

The modulation methodology is at the beginning of its development, therefore performing tests using well known reactions are necessary to assess the working procedures, limits and possibilities of this method. This work presents as a *proof of concept* the use of concentration-modulation excitation spectroscopy (c-MES) to investigate the reaction mechanism during the reverse water gas shift reaction on a model gallium oxide-supported palladium catalyst.

2. Experimental

2.1. Catalyst and experimental setup

Pure γ-Ga_2O_3 phase was synthesized following the procedure reported elsewhere [17]. Hydrated gallium hydroxide gel was obtained from the addition of an ammonia ethanolic solution (14 wt.%) to a solution of $Ga(NO_3)_3{\cdot}9H_2O$ in ethanol. This gel was filtered and washed with ethanol at room temperature. The resulting material was dried at 343 K (8 h) and then air calcined at 773 K (5 h). A γ-Ga_2O_3 polymorph with S_{BET} value equal to 105 $m^2\,g^{-1}$ was obtained.

Pd(1 wt.%)/γ-Ga_2O_3 was prepared by incipient-wetness impregnation using $Pd(OAc)_2$ (Sigma) in acetone, with further drying/calcining in air (673 K, 2 h), H_2 reduction (2% H_2/Ar, 723 K, 2 h) and passivation with oxygen pulses at room temperature. As reported recently, this activation procedure produces partial alloy of the palladium particles with reduced gallium (Pd–Ga bimetallic particles), herein referred to as Pd(Ga)/Ga_2O_3 catalyst [18].

The experimental setup consisted of a high-temperature reaction DRIFTS cell (Harrick) fitted with KBr windows. The reaction flow was going down through the reactor bed, so that the upper layer of the catalyst, approximately 200 μm, is probed by IR beam in the front of the bed. The amount of catalyst used in the DRIFTS cell was 25 mg, with a bed height of about 5–7 mm. The cell was connected to the feed gas cylinders through low-volume stainless-steel lines. Rapid exchange of the gas composition was performed by switching an electronically actuate flow-through valve (Vici-Valco Instruments), which avoids pressure drop during changes, synchronized with the FTIR spectrometer. The gas flows were adjusted by mass flow controllers.

The DRIFT cell was mounted inside the sample compartment of the FTIR spectrometer (Thermo-Electron, Nicolet 8700 with a cryogenic MCT detector). The bench of the spectrometer was continuously purged with dried air (Parker Balston FTIR purge gas generator) to eliminate CO_2 and water vapor contributions to the spectra. Time-domain IR spectra were recorded in kinetic and rapid-scan mode at a resolution of 4 cm^{-1}. The reference spectrum was collected without catalyst.

Previous to the c-MES experiments, the catalyst was activated by heating to 523 K at 5 K/min under H_2 (100 cm^3/min). After 30 min at this last temperature the flow was switched to pure Ar (100 cm^3/min) and kept for another 30 min at 523 K. A similar treatment was applied to the bare Ga_2O_3 support but at 623 K in order to clean the surface from carbonate residues.

After recording the background spectrum, a modulation experiment was started by varying the inlet mass flow of the reaction gas using the desired modulation frequency. After waiting at least five modulation periods to allow for an adjustment of the system to the external perturbation, the recording of the spectra was started. At least 125 spectra in each c-MES period were acquired, using reactant exchange frequencies from 1.7 to 33 mHz.

2.2. Modulation excitation spectroscopy with phase sensitive detection (MES-PSD)

The periodic variation of an external parameter affecting an operating system under *ss* condition allows the selective observation of a chemical or physical phenomenon by distinguishing the active-intermediate from the spectator ones. If a catalytic system is perturbed by a periodic stimulation, all the parameters in the system, which are affected by this perturbation, will also change periodically at the same frequency as the stimulation or their harmonics, but with a phase delay (φ) [12–14]. Further analysis of the obtained information can be achieved by demodulation of the oscillating response signal, $A(t)$, using a so-called phase sensitive detection (PSD) method developed by Baurecht and Fringeli [12], as shown in Eq. (1):

$$A(\phi_k^{PSD}) = \frac{2}{T}\int_0^T A(t)\ \sin(k\omega t + \phi_k^{PSD})dt \quad (1)$$

where, T is the length of one period, ω is the stimulation frequency, k is the demodulation index, ϕ_k^{PSD} is the demodulation phase angle for $k\omega$ demodulation, and $A(t)$ and $A(\phi^{PSD})$ are the active species response in time- and phase-domain, respectively. In other words Eq. (1) transforms time-domain spectra, $A(t)$, into phase-resolved spectra, $A_k(\phi_k^{PSD})$.

The PSD method possesses the following advantages: (i) the spectra in the phase domain allow to distinguish and separate easily static signals from the changing ones, that is, spectator from active intermediate species; (ii) the signal-to-noise ratio in the spectra improves; and (iii) the delays in the signals of different active species, which are due to the reaction mechanism, are better resolved in the phase-domain than in time-domain.

The phase delays from different signals (e.g. intermediate species) can be accurately determined by PSD, that is, the in-phase angle value of ϕ^{PSD} at which the amplitude reaches a maximum. The phase delays and the amplitudes of the signals in the phase-domain contain kinetic information of the system, and the dynamic behavior can be studied. Then, based on the φ values, species with different kinetics can be separated and insights into the catalytic mechanism can be addressed.

As it was shown by Baurecht and Fringeli [12], the phase-domain response can be derived analytically for a harmonic stimulation from Eq. (1) as follows:

$$A(\bar{\nu}, \phi^{PSD}) = A\cos(\varphi - \phi^{PSD}) \quad (2)$$

where $\bar{\nu}$ stands for wavenumber (cm^{-1}).

Then the amplitude $A(\bar{\nu}, \phi^{PSD})$ becomes maximum for $(\varphi - \phi^{PSD}) = 0^\circ$ or 360°, which is called 'in-phase' angle, and minimum (negative) for $(\varphi - \phi^{PSD}) = 180^\circ$, which is the 'out-phase' angle, and it is zero for $(\varphi - \phi^{PSD}) = 90^\circ$ or 270°. Therefore, actual (or apparent) phase delay, φ, which has the kinetic information of the observed process, can be calculated [12]. Moreover, the use of square-wave stimulation (generated in our MES experiments by switching the admission valve) has the advantage of allowing to obtain phase lags of higher frequencies from a single square-wave experiment. Thus, values of φ at higher stimulation frequencies, 1ω, 3ω, 5ω,... are acquired by a single experiment with a square-wave stimulation at 1ω [19]. In practice, we only use 1ω and 3ω due to the loss of signal-to-noise ratio at higher frequencies.

The dome of the DRIFT cell, previous to the catalyst bed, behaves as a Continuous Stirred Tank Reactor (CSTR) system with a residence time, $\tau = V/F$, where V is the volume of the cell = 18 cm^3, and F is the volumetric flow. Therefore, the residence time can be used to "buffer" the amplitude of the perturbation (concentration of reactants) into the cell. Thus, generating square-wave perturbations by means of switching between two reactants, a reaction mixture at

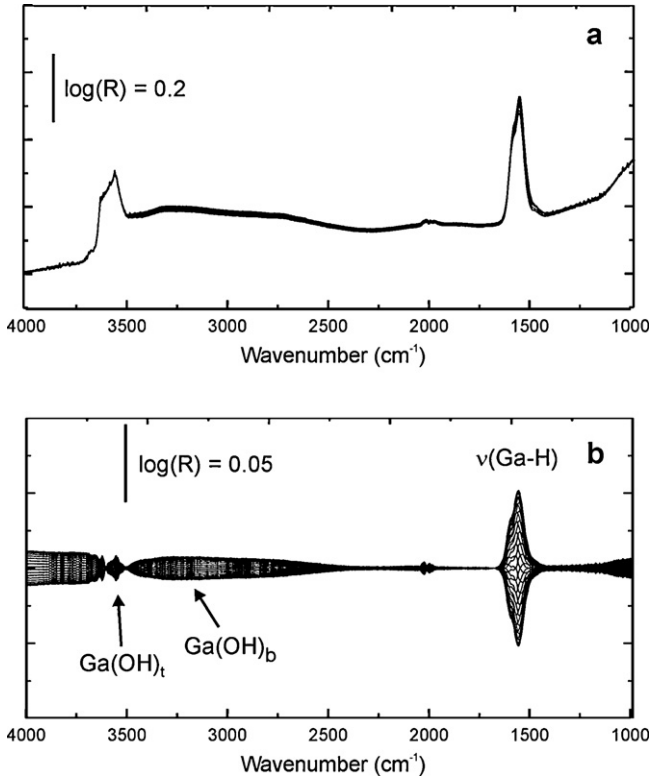

Fig. 1. (a) Time-domain DRIFT spectra during a c-MES cycle H_2–Ar over Ga_2O_3 (100 ml min^{-1}, 523 K, ω = 4.2 mHz); (b) phase-domain spectra after PSD demodulation.

steady state can be reached when the applied frequency tends to infinity.

3. Results and discussion

3.1. Hydrogen and carbon dioxide adsorption and reaction on Ga_2O_3

Time-domain spectra shown in Fig. 1a allow identifying the rise of a couple of overlapped bands at around 2000 cm^{-1} during H_2/Ar exchanges into the DRIFT cell at 523 K. As shown previously by some of us, after the adsorption of H_2 (or D_2) on pure gallium oxides, two overlapped signals owing to the Ga–H stretching vibration are observed by infrared spectroscopy, and their relative intensities depend on the surface coordination of the partially reduced surface gallium cations ($Ga^{\delta+}$): one at 2003 cm^{-1}, is assigned to the Ga—H bonds on the gallium cation in the tetrahedral sites, while the other at 1980 cm^{-1}, corresponds to H bonded to a gallium cation in an octahedral position [17,20].

Phase-domain spectra, after PSD demodulation, are presented in Fig. 1b. Spectrum clearly shows a synchronous correlation between the Ga—H signals at 2003 and 1980 cm^{-1} and a broad band corresponding to bridged O—H bonds, broad at 3600 cm^{-1} (HO_b) and part of the terminal Ga—OH, peak at 3550 cm^{-1}. This result indicates a heterolytic adsorption of H_2 on Ga—O—Ga sites, producing Ga—H and an additional OH group over the gallium oxide surface.

$$H_2 + Ga{-}O{-}Ga \rightarrow Ga^{\delta+}{-}H^{\delta-} + Ga{-}OH$$

Modulated adsorption of CO_2 was investigated in a range of temperatures, due to the different adsorption heats of the bicarbonate/carbonates on gallium oxides.

To obtain a more detailed picture of the CO_2 chemisorption on the gallium oxide surface, it is necessary to identify the

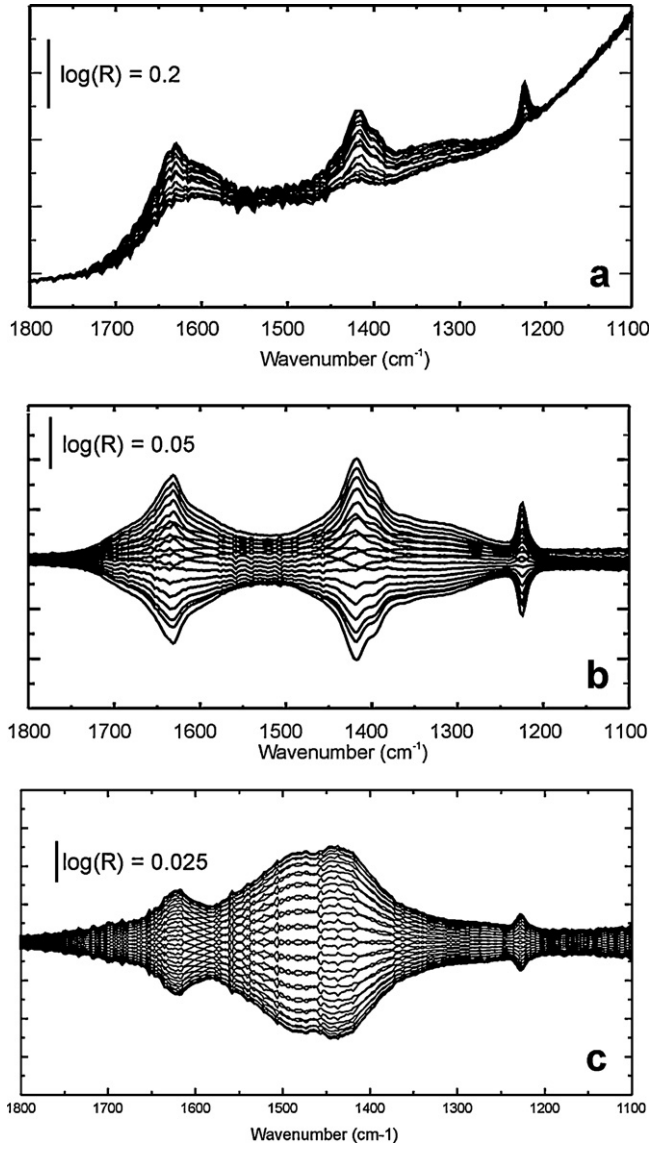

Fig. 2. (a) Time-domain DRIFT spectra during a c-MES cycle CO_2–Ar over Ga_2O_3 (100 ml min^{-1}, 323 K, ω = 4.2 mHz); (b) phase-domain spectra after PSD demodulation (323 K); (c) phase-domain spectra after PSD demodulation (523 K).

carbonate groups, and their fractional surface composition and thermal stability. The right assignment of the IR bands to surface carbonate species is supported by the pertinent analyses of the following features [21]: (i) the wavenumber of the IR signals corresponding to carbonates adsorbed over other metal oxides, (ii) the width of the $\Delta\nu$-band splitting of the CO_3 anion (that is, the $\Delta\nu = \nu_{as} - \nu_s$ of the CO_3 stretching modes) due to the loss of its D_{3h} symmetry by chemisorption, and (iii) the thermal evolution of the intensity of each signal (thermal stability). For details in the assignment of (bi)carbonate modes on gallium oxides, please, see Ref. [22].

At 323 K, Fig. 2a and b, mostly bicarbonate groups are formed upon chemisorption of CO_2 on the most basic hydroxyl groups: mono (m-HCO_3^-) and bidentate (b-HCO_3^-) [$\nu_{as}(CO_3)$ = 1632 cm^{-1}; $\nu_s(CO_3)$ = 1400 or 1418 cm^{-1} (for m- or b-); $\delta(OH)$ = 1225 cm^{-1}]. Together with the bicarbonate groups, IR bands assigned to bridge carbonate [$\nu_{as}(CO_3)$ = 1680 cm^{-1}; $\nu_s(CO_3)$ = 1315 cm^{-1}], bidentate carbonate [$\nu_{as}(CO_3)$ = 1587 cm^{-1}; $\nu_s(CO_3)$ = 1360 cm^{-1}],

and polydentate/monodentate carbonate [$\nu_{as}(CO_3) = 1460\,cm^{-1}$; $\nu_s(CO_3) = 1406\,cm^{-1}$] species developed [22]. Polydentate and monodentate carbonate groups have similar band positions and $\Delta\nu_3 < 100\,cm^{-1}$ [21,22]. They can only be distinguished by their thermal stability, been p-CO_3^{2-} more stable than m-CO_3^{2-}. At increasing adsorption temperature, most of the carbonate species lost intensity, except for polydentate carbonates, which remained on the surface even at 723 K.

MES experiments carried out at 523 K (RWGS reaction temperature) are shown in Fig. 2c. Weak bands due to bicarbonate [$\nu_{as}(CO_3) = 1632\,cm^{-1}$; $\nu_s(CO_3) = 1430$; $\delta(OH) = 1225\,cm^{-1}$] and polydentate/monodentate carbonate [$\nu_{as}(CO_3) = 1485\,cm^{-1}$; $\nu_s(CO_3) = 1430\,cm^{-1}$] were recorded.

As shown above, pure gallium oxide is able to dissociatively chemisorb H_2, given rise to Ga—H surface species. These surface hydrides are reactive and can hydrogenate carbonates. CO_2/H_2 reaction was investigated in the bare support. DRIFT spectra taken under steady state (after 30 min of reaction) during flow of H_2/CO_2 (1:1) at 523 K showed the rise of several peaks emerged in the 3000–2800 cm^{-1} and 1700–1200 cm^{-1} regions typical of formate groups (HCOO), along with the already identified bands of carbonates and Ga—H.

To assign and further investigate the role of this species in the reaction mechanism, c-MES experiments were carried out over the Ga_2O_3 sample at 523 K flowing alternatively H_2/CO_2 (1:1) or Ar and H_2 or CO_2 in a range of frequencies. Time-domain and phase-domain spectra exchanging $H_2 + CO_2$(1:1) to Ar are shown in Fig. 3a and b, respectively. Experiments changing H_2 or CO_2 are present in Supplementary Material.

Time-domain spectra showed very small changes in the carbonates and formate bands over time. The periodic variations of the signal intensities, which are due to the concentration modulation, are hard to read from these spectra. To further analyze these data, the PSD method was applied to the spectra. Demodulated IR spectra permit easily identify the synchronous change of bands due to carbonates around 1400 cm^{-1}, and Ga—H species at 1980/2003 cm^{-1}. Also, very weak signals of carbon monoxide in the gas phase (2175–2100 cm^{-1}) produced by the RWGS reaction are now detectable. Moreover, a fingerprint identification of formate species with different surface coordination could be achieved after PSD demodulation: monodentate formate (m-HCOO) [$\nu_{as}(OCO) = 1640\,cm^{-1}$, $\delta(CH) = 1309\,cm^{-1}$, $\nu_s(OCO) = 1272\,cm^{-1}$], bridged formate (br-HCOO) [$\nu_{as}(OCO) = 1580\,cm^{-1}$, $\delta(CH) = 1382\,cm^{-1}$, $\nu_s(OCO) = 1362\,cm^{-1}$], and bidentate formate (b-HCOO) [$\nu_{as}(OCO) = 1600\,cm^{-1}$] (see Fig. 2 in Supplementary Material). Details of the assignment of each observed vibrational mode for formate groups with different surface coordination combining DFT calculation and infrared experiments with isotopic labeling can be found in Ref. [23].

It is worth noting here that infrared spectra acquired using the MES-PSD approach allow fingerprint identification of carbonaceous species (HCOO and CO_3^{2-}) based on their C—O stretching modes during reaction, which are sensitive to the surface coordination of such molecules. Conversely, previous reports employing DRIFT-SSITKA experiments (using $^{13}CO_2/^{12}CO_2$ exchange) transient analysis of the formate groups was performed on the basis of ν(C—H) signals, which are difficult to correlate to a single formate species, as a result of the high background present in the carbonate region and the complexity of this band structure [24]. This difficulty can be overcome after demodulation by PSD algorism of c-MES spectra and detailed information about the reactivity of each formate groups can be achieved as will be shown next.

C-MES experiments showed that carbonate species at 1413–1400 cm^{-1} are, as expected, in-phase with the change in the CO_2(g) partial pressure, while, Ga—H and formates are in-phase with the H_2(g) (see also Fig. 3 in Supplementary Material). Bridged formate presents signals of high intensity in the time-domain spectra, most of which are only slightly affected by the modulation of reactants, and therefore became small in the phase-resolved spectra after PDS demodulation (Fig. 3a and b). Conversely, monodentate formate species are almost undetectable in the time-domain spectra, but are easily seen in the phase-domain spectra.

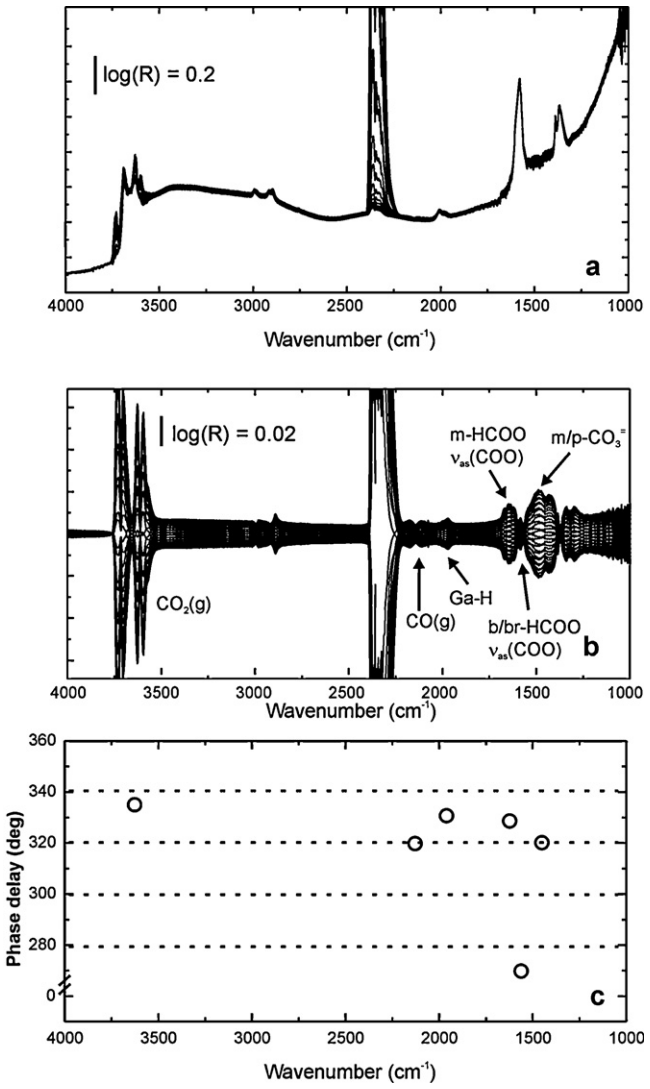

Fig. 3. (a) Time-domain DRIFT spectra during a c-MES cycle CO_2/H_2–Ar over Ga_2O_3 (100 ml min^{-1}, 523 K, ω = 4.2 mHz); (b) phase-domain spectra after PSD demodulation; (c) phase delay (φ) for selected bands of: CO_2(g) (3600 cm^{-1}), Ga—H (1980 cm^{-1}), m/p-CO_3 = (1400 cm^{-1}), b-/br-HCOO (1600/1580 cm^{-1}), m-HCOO (1640 cm^{-1}) and CO(g) (2175 cm^{-1}).

Phase-resolved spectra allow following, selectively, the different reactivity of formate species. Fig. 3c shows the phase delay (φ, that is, ϕ^{PSD} at maximum amplitude) for some characteristic infrared signals of: CO_2(g) (3600 cm^{-1}), Ga—H (1980 cm^{-1}), m/p-CO_3^{2-} (1400 cm^{-1}), b-/br-HCOO (1600/1580 cm^{-1}), m-HCOO (1660 cm^{-1}) and CO(g) (2175 cm^{-1}). An analysis of the phase lag of each surface species indicates that m-HCOO are rapidly formed and decomposed to CO, while br-/b-HCOO seems to have a much lower reaction rate, $\varphi = 325^\circ$ vs. $\varphi = 250^\circ$, respectively.

CO_2 hydrogenation has been extensively investigated using homogeneous catalyst such as aluminum and lithium hydrides [25,26]. The reaction proceeds through the insertion of the hydride

of metal transition complex into the electrophilic carbon atom of the CO_2 molecule to produce a formate intermediate:

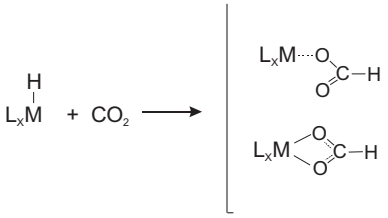

The Schwartz reactive, $Cp_2Zr(H)(Cl)$ [$cp = \eta^5$-C_5H_5], has also been used as a model system to study this reaction [27–29]. The reaction mechanism is described as a concerted process, where the CO_2 molecule forms an M—O bond while the hydride is transferred to the carbon atom [26]:

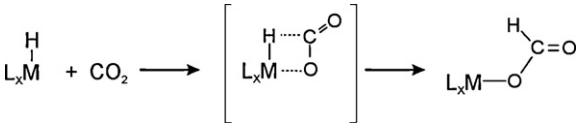

As well, carbonate and carboxylate intermediates have been suggested, for instance, with the complex $RhCl[P(C_6H_5)_3]_3$ [26].

In this heterogeneously catalyzed reaction occurring on the gallium oxide surface, carbonates groups, particularly m/p-CO_3^{2-}, are hydrogenated to formates via a nucleophilic attack by gallium hydride:

$$CO_3^{2-} + Ga{-}H \rightarrow HCOO$$

Later on, to complete the reaction cycle, formates are decomposed into CO(g) and surface hydroxyl group (Ga—OH), the last one should react to release water. The reverse reaction, that is the insertion of CO(gas) into a Ga—OH surface group has been previously investigated by some of us [30]:

$$CO(g) + Ga{-}OH \rightarrow HCOO{-}Ga.$$

Monodentate formate seems to be the most reactive intermediate, while bridged and bidentate accumulates on the surface and react slowly.

3.2. C-MES investigation of the CO_2 hydrogenation on $Pd(Ga)/Ga_2O_3$

Concentration-modulation experiments were performed on a $Pd(Ga)/Ga_2O_3$ catalyst. Hydrogen and carbon dioxide adsorption showed the same results than on the bare support (spectra not shown). More interesting, the RWGS reaction was performed on this system and DRIFT spectra were collected under steady state and during periodic variation of the reactant partial pressure. DRIFT spectra registered under RWGS reaction conditions ($H_2/CO_2 = 1/1$, 523 K) over $Pd(Ga)/Ga_2O_3$ presented several, convoluted, features in the 1700–1100 cm^{-1} region. To distinguish and characterize the role of each surface species in the reaction mechanism, periodic modulation of the gas composition was applied at increasing frequencies (decreasing amplitudes).

Fig. 4a and b shows, as an example, the time-domain DRIFT spectra during a complete cycle of H_2/CO_2 to Ar and phase-domain spectra, after demodulation, for a complete period, that is, for ϕ^{PSD} between 0 and 360°, each 10°. Complementary experiments changing H_2 to CO_2 are present in Supplementary Material.

After demodulation, the periodic signals in the phase-resolved spectra are the only remaining signals in the spectra (Fig. 4b). This is a direct consequence of the separation of the static signals from the periodic ones by PSD. Then, a clear distinction among

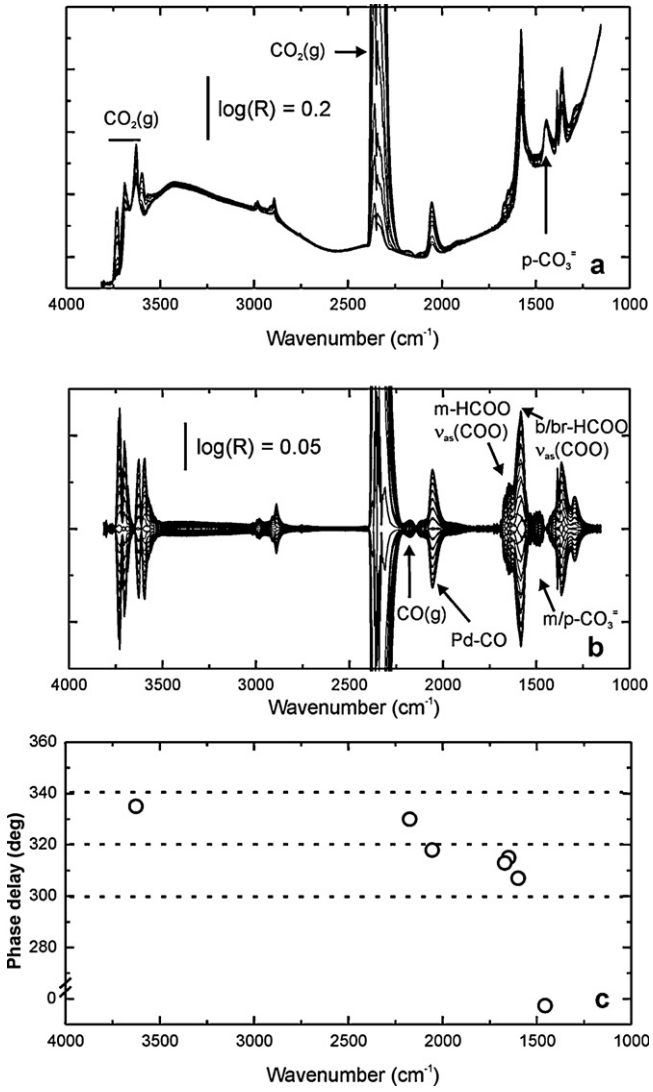

Fig. 4. (a) Time-domain DRIFT spectra during a c-MES cycle CO_2/H_2–Ar over Pd/Ga_2O_3 (100 ml min^{-1}, 523 K, ω = 4.2 mHz); (b) phase-domain spectra after PSD demodulation; (c) phase delay (φ) for selected bands of: CO_2(g) (3600 cm^{-1}), Pd–CO (2056 cm^{-1}), m/p-CO_3 = (1400 cm^{-1}), b-/br-HCOO (1600/1580 cm^{-1}), m-HCOO (1640 cm^{-1}) and CO(g) (2175 cm^{-1}).

infrared signals due to m-/p-carbonate (1450–1300 cm^{-1}), b-/br-HCOO (1600/1580 cm^{-1}), and m-HCOO (1660 cm^{-1}), and carbon monoxide in gas phase (P and Q roto-vibrational branches) and linearly adsorbed on the (Pd/Ga) metal particles, Pd—CO (2056 cm^{-1}) can be done.

Fig. 4c shows the phase delay (φ) for characteristic infrared signals of: CO_2(g) (3600 cm^{-1}), CO(g) (2175 cm^{-1}), Pd—CO (2056 cm^{-1}), m/p-CO_3^{2-} (1400 cm^{-1}), b-/br-HCOO (1600/1580 cm^{-1}), and m-HCOO (1660 cm^{-1}). As observed on the bare support, analysis of the evolution of peak intensity indicates that m/p-CO_3^{2-} are hydrogenated to monodentate, bridged, and bidentate formate species. Formate groups are decomposed to release CO to the gas phase, part of which could re-adsorb into the metal particles. However, RWGS can also proceed efficiently over Pd or Pd–Ga sites [18,31] by means of an independent route without participation of the support. PSD analysis in Fig. 4c shows that phase lag of adsorbed CO, Pd—CO (φ = 318°), is slightly higher than the one of formates, particularly of m-HCOO (φ = 313°). This suggests that Pd—CO is mainly produced by reaction between CO_2 and H_2 on the metal particles, rather than re-adsorbed from the gas phase.

Comparing the intensity of the infrared bands of intermediates registered on Pd/Ga_2O_3 vs. Ga_2O_3, more intense bands due to hydrogenated intermediates, e.g. HCOO, are present on the supported metal catalyst. Thus, the hydrogenation of surface carbonates to formate intermediates is more efficient in the presence of metal particles. Activity measurements taken under steady state condition (20 h) showed that rate of CO production was 3.6×10^{-7} mol s^{-1} g^{-1} on Pd/Ga_2O_3. Likewise, the CO production based on metal sites (turn-over frequency: TOF) was almost 10-fold higher using Pd/Ga_2O_3 vs. Pd/SiO_2 (that is, palladium supported on an "inert" support). Thus, most of the RWGS reaction is carried out via a bifunctional mechanism involving both the metal particles and the gallia support. The highest production of CO in the Ga_2O_3 is a consequence of the efficient supply of atomic hydrogen via a spillover mechanism from the palladium metal particles [19,32]

Hydrogenation of carbonaceous intermediates, e.g. carbonates and formates, on bifunctional catalysts based on metal particles supported on metal oxides via hydrogen spillover has been widely discussed in the literature [33,34]. For instance, Jung and Bell [35] using Cu/ZrO_2 and Kalies et al. [36] using Pt/ZrO_2, showed that CO_3^{2-} species are hydrogenated to HCOO by hydrogen provided by the metal function. A detailed study of the CO_2 hydrogenation to methanol, as well as methanol decomposition, on a model Pd/gallia catalysts have been previously conducted, mainly by means of transmission in situ FTIR [37,38]. It was shown that this system works as a true bifunctional system where carbonaceous intermediates chemisorbed onto gallia are successively hydrogenated to methanol by hydrogen supplied via spillover from the palladium metal particles. A work using physical mixtures of Ga_2O_3/SiO_2 and Pd/SiO_2 demonstrated that atomic hydrogen, H_S, was generated at the silica-supported Pd particles and moved (spilled over) to the supported gallia ones, where the carbonaceous species were then hydrogenated [32]. Therefore, the higher concentration of surface hydrogen, H_S, on the gallium oxide, provided by the metal particles via a spillover mechanism, allowed a more efficient hydrogenation of carbonates to formates.

Concerning the reactivity to each formate groups, a careful analysis of the phase delay after the PSD treatment of the spectra shows that stability follows this order: m-HCOO ($\varphi = 315°$) < b-HCOO ($\varphi = 307°$) < br-HCOO($\varphi = 303°$). These experimental results are in agreement with previous DTF calculations carried out on (1 0 0)β-Ga_2O_3 [23]. There, the barriers for the interconversion of the different formate species (e.g. monodentate, bidentate and bridged) have been calculated. It was found that m-HCOO can change coordination to form bidentate and bridged formate, which are the most stable species.

The role of fast and/or slow formate species in the direct and reverse WGS reaction have been addressed by some authors. Burch et al. [24] conclude that formates are spectators, or at the best, a minor route in metal (Pt, Au) supported on CeO_2 and related oxides. However, a very recent review from the same research group indicates that the true contribution of formate in the WGS mechanism remain controversial [39].

Investigation of the RGWS reaction on the $Pd–Ga_2O_3$ system by means of c-MES experiments coupled with PDS analysis, allows us to conclude that monodentate formate on the gallia surface are the most active intermediates, while bridged and bidentate formates seem to be slower intermediates.

4. Conclusions

Experiments of concentration-modulation excitation spectroscopy (c-MES) coupled with phase sensitive detection (PSD) method using *operando* DRIFT were performed to investigate the reverse water gas shift reaction on a model Pd(1 wt.%)/γ-Ga_2O_3 catalyst. This methodology allowed the selective identification of infrared signals of active reaction intermediates.

The results showed that hydrogen can be dissociatively chemisorbed by gallium cations, giving Ga–H surface species, which can hydrogenate carbonate groups, formed by CO_2 adsorption, to formate species with different coordination, e.g. monodentate, bidentate and bridged. The hydrogenation step is more efficient when metal particles are present because of the higher concentration of hydrogen in the surface via a spillover mechanism. It is suggested that monodentate formate is the most reactive (fast) intermediate, while bidentate and bridged are more stable (slow) intermediates.

Acknowledgments

Financial support from the Consejo Nacional de Investigaciones Científicas y Técnicas (CONICET), Universidad Nacional del Litoral (UNL) CAID J379 and the Agencia Nacional para la Promoción de la Ciencia y Tecnología of Argentina (ANPCyT) PICT-729 and PME-611 is gratefully acknowledged. We thank Dr. A.L. Bonivardi and Lic. D. Lesa for the preparation of the Pd/γ-Ga_2O_3 catalyst.

Appendix A. Supplementary data

Supplementary data associated with this article can be found, in the online version, at http://dx.doi.org/10.1016/j.cattod.2012.08.020.

References

[1] M.A. Bañares, M.O. Guerrero-Perez, J.L.G. Fierro, G.J. Garcia Cortez, Journal of Materials Chemistry 12 (2002) 3337–3342.
[2] F.C. Meunier, A. Goguet, S. Shekhtman, D. Rooney, H. Daly, Applied Catalysis A-General 340 (2008) 196–202.
[3] R. Brosius, P. Bazin, F. Thibault-Starzyk, J.A. Martens, Journal of Catalysis 234 (2005) 191–198.
[4] A. Vimont, F. Thibault-Starzyk, M. Daturi, Chemical Society Reviews 39 (2010) 4928–4950.
[5] J.C. Clark, S. Dai, S.H. Overbury, Catalysis Today 126 (2007) 135–142.
[6] Y. Denkwitz, B. Schumacher, G. Kucerová, R. Behm, Journal of Catalysis 267 (2009) 78–88.
[7] A. El-Moemen, A. Karpenko, Y. Denkwitz, R. Behm, Journal of Power Sources 90 (2009) 64–69.
[8] G. Jacobs, S. Ricote, B. Davis, Applied Catalysis A-General 302 (2006) 14–21.
[9] F. Meunier, D. Reid, A. Goguet, S. Shekhtman, C. Hardacre, R. Burch, W. Deng, M. Flytzani-Stephanopoulos, Journal of Catalysis 247 (2007) 277–287.
[10] F. Meunier, Catalysis Today 155 (2010) 164–171.
[11] J.S.J. Hargreaves, D. Jackson, G. Webb (Eds.), Isotopes in Heterogeneous Catalysis, Catalytic Science Series, vol. 4, Imperial College Press, London, 2006.
[12] D. Baurecht, U.P. Fringeli, Review of Scientific Instruments 72 (2001) 3782–3792.
[13] D. Baurecht, I. Porth, U.P. Fringeli, Vibrational Spectroscopy 30 (2002) 85–92.
[14] A. Urakawaa, T. Bürgi, A. Baiker, Chemical Engineering Science 63 (2008) 4902–4909.
[15] E.E. Ortelli, J. Wambach, A. Wokaun, Applied Catalysis A-General 192 (2000) 137–152.
[16] E.E. Ortelli, J. Wambach, A. Wokaun, Applied Catalysis A-General 216 (2001) 227–241.
[17] S.E. Collins, M.A. Baltanás, A.L. Bonivardi, Langmuir 21 (2005) 962–970.
[18] S.E. Collins, J.J. Delgado, C. Mira, J.J. Calvino, S. Bernal, D.L. Chiavassa, M.A. Baltanás, A.L. Bonivardi, Journal of Catalysis 292 (2012) 90–98.
[19] A. Urakawa, T. Burgi, A. Baiker, Chemical Physics 324 (2006) 653–658.
[20] S.E. Collins, J.L.G. Fierro, M.A. Baltanás, A.L. Bonivardi, Journal of Catalysis 211 (2002) 252–264.
[21] G. Busca, V. Lorenzelli, Journal of Materials Chemistry 7 (1982) 89–126.
[22] S.E. Collins, M.A. Baltanás, A.L. Bonivardi, Journal of Physical Chemistry B 110 (2006) 5498–5507.
[23] M. Calatayud, S.E. Collins, M.A. Baltanás, A.L. Bonivardi, Physical Chemistry Chemical Physics 11 (2009) 1397–1405.
[24] A. Goguet, F.C. Meunier, D. Tibiletti, J.P. Breen, R. Burch, Journal of Physical Chemistry B 108 (2004) 20240–20246.
[25] R.F. Nystrom, W.H. Yanko, W.J. Brown, Journal of the American Chemical Society 70 (1948) 441.
[26] P. Jessop, T. Ikariya, R. Noyori, Chemical Reviews 95 (1995) 259–272.
[27] A. Cutler, M. Raja, A. Todaro, Inorganic Chemistry 26 (1987) 2877–2881.
[28] T. Bodnar, E. Coman, K. Menard, Inorganic Chemistry 21 (1982) 1275–1277.

[29] S. Gambarotta, S. Strologo, C. Floriati, A. Chiesi, C. Guastini, Journal of the American Chemical Society 107 (1985) 6278–6282.
[30] S.E. Collins, M.A. Baltanás, A.L. Bonivardi, Journal of Molecular Catalysis A: Chemical 281 (2008) 73–78.
[31] A. Haghofer, K. Föttinger, F. Girdsdies, D. Teschner, A. Knop-Gerike, R. Schlögl, G. Rupprechter, Journal of Catalysis 286 (2011) 13–21.
[32] S.E. Collins, D.L. Chiavassa, A.L. Bonivardi, M.A. Baltanás, Catalysis Letters 103 (2005) 83–88.
[33] W.C. Conner, S.J. Teichner, G.M. Pajonk, Advances in Catalysis 34 (1986) 1–79.
[34] W.C. Conner, J.L. Falconer, Chemical Reviews 95 (1995) 759–788, and references therein.
[35] K.-D. Jung, A.T. Bell, Journal of Catalysis 193 (2000) 207–223.
[36] H. Kalies, N. Pinto, G.M. Pajonk, D. Bianchi, Applied Catalysis A: General 202 (2000) 197–205.
[37] S.E. Collins, M.A. Baltanás, A.L. Bonivardi, Journal of Catalysis 226 (2004) 410–421.
[38] S.E. Collins, M.A. Baltanás, A.L. Bonivardi, Applied Catalysis A-General 295 (2005) 126–133.
[39] R. Burch, A. Goguet, F.C. Meunier, Applied Catalysis A-General 409–410 (2011) 3–12.